

2020 Numisheet benchmark study uniaxial tensile tests summary

Evan Rust, William E. Luecke, Mark A. Iadicola¹

29 April 2020

1. Introduction

This report describes the test equipment, process, analysis, and data file formats for the 2020 Numisheet benchmark study tensile testing of the four materials associated with the Numisheet conference benchmarks. The four materials include two steel alloys, DP980 for Benchmark 1 and DP1180 for Benchmark 2, and two 6000 series aluminum alloys, AA6xxx-T4 for Benchmark 1 and AA6xxx-T81 for Benchmark 2, that will be referred to here as BM1-DP980, BM2-DP1180, BM1-6xxx-T4, and BM2-6xxx-T81, respectively. The testing reported here was requested by the 2020 Numisheet Benchmark Committee and was performed by the Center for Automotive Lightweighting (NCAL) in Gaithersburg, MD. The tests were performed at NCAL from October 2019 through January 2020. The summary table file, “Numisheet 2020 Uniaxial Tension Test Summary Table.csv”, contains the names of each data file with key aspects of each test noted (see Table 2. Column descriptions for tensile test summary table file (“Numisheet 2020 Uniaxial Tension Test Summary Table.csv”).). The data files described below contain the processed results of Digital Image Correlation (DIC) measurements, and therefore this report describes the basis for the parameters used for the DIC analyses. This report and the described data files are available at doi:10.18434/M32202.

NOTE: In the summary table file and occasionally in this report there are unique identifiers used by the NCAL database to identify specific tests or specimens. These are included so that any future inquiries regarding specific test results can be efficiently traced back to the raw data files, images, stereo-DIC system hardware, calibrations used, etc. These identifiers typically follow the format A#####-AAA-### (potentially followed by additional numbers and letters) where the leading “A” could be “L”, “E”, or “S”. In this report, these numbers will be delineated using a separate sans-serif font and brackets, e.g., [L191210-WEL-001].

2. Test Methods

The uniaxial tension tests were performed using a universal testing machine in the NCAL laboratory in accordance with the ASTM E8 standard [2]. The testing machine has a lower moving hydraulic actuator and a fixed upper crosshead where the loadcell is attached. Each specimen was taken to fracture of the specimen into two pieces. The face of the test specimen, across the width and along the reduced parallel section, is measured throughout the test using a stereo-DIC system. Tests were performed with specimens fabricated from the sheet material at every 15° increment from the rolling direction to 90° to the rolling direction. For each orientation and material three repeat tests were performed. In this report, the results for all the tests are reported including each repeat test; there is no averaging between the repeat tests.

2.1. Specimen

Figure 1 shows the ASTM E8 rectangular tension test specimen geometry used for these tests. Reported dimensions are the average of three measurements made on the center and at each end of the reduced

¹ please direct all questions regarding this data and report to Mark Iadicola: mark.iadicola@nist.gov

parallel section of the test specimen. The specimens were fabricated with an abrasive waterjet cutter from sheet material.

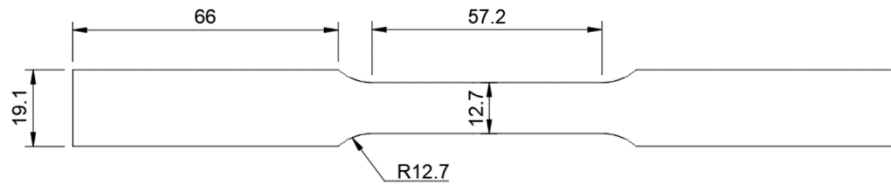


Figure 1: ASTM E8 [2] rectangular tension test specimen used for uniaxial testing (nominal dimensions in mm).

2.2. Mechanical testing equipment

Figure 2 shows the testing machine and the location of DIC cameras and lighting. The testing machine alignment met ASTM E1012 Class 5. [1]

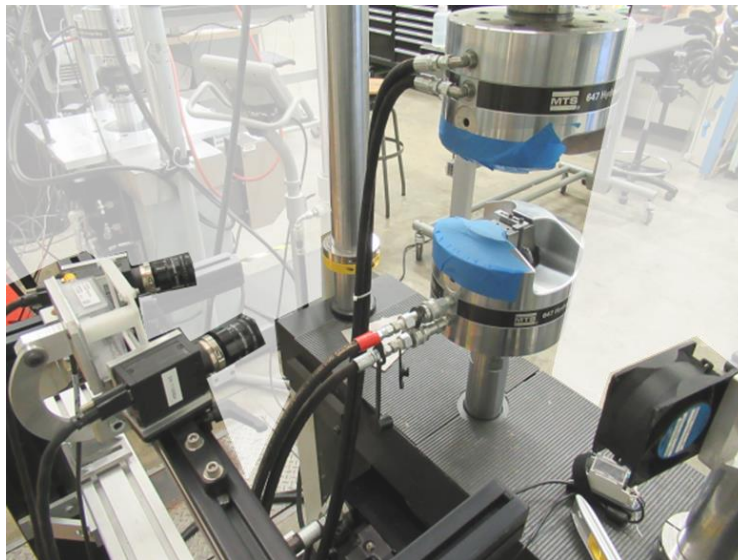


Figure 2: NIST uniaxial tension testing machine with stereo DIC camera system.

2.3. Test Protocol

Each test consists of two segments: a ramp in force control to bring specimen to zero force followed by a tension ramp in displacement control until the specimen fractures. In most tests the image acquisition rate was 2 images per second during the initial elastic loading segment, and then 1 image per second for the subsequent plastic portion. Relevant test details are:

Actuator velocity: 0.855 mm/min

Nominal strain rate: 0.015 mm/mm/min = 0.00025mm/mm/s (ASTM E8 standard rate)

2.4. DIC test equipment and analysis

The local strains in the test specimen are measured using digital image correlation from a speckle pattern applied to the face of the test specimen. To create the speckle pattern, the specimen is spray painted with a matte white base coat, then a matte black paint is sprayed from one meter away onto the specimen until approximately 50 % of the specimen is covered in black paint. The resulting pattern features are on

average approximately 4 pixel in size (based on a line intercept method with a minimum intensity difference of 50 gray levels) or approximately 150 μm . The table in Section 4.4 summarizes the relevant features of the digital image correlation equipment for the tests, as recommended by the International Digital Image Correlation Society (iDICs) A Good Practices Guide for DIC [3]. All DIC analyses used Correlated Solutions² Vic-3D 8.2.4 build 525 digital image correlation software. A sensitivity study yielded optimal DIC analysis parameters (see Section 4.5 for details). These parameters changed slightly between tests due to changes of camera positioning between materials tested. The strain noise floor (see Section 4.6) for each test is included in the summary table file (“Numisheet 2020 Uniaxial Tension Test Summary Table.csv”). For most of the tests, the Hencky true strain noise floors were approximately ϵ_{yy} : 200 $\mu\text{m}/\text{mm}$ and ϵ_{xx} : 250 $\mu\text{m}/\text{mm}$.

In all analyses, the coordinate system origin is positioned at the center of the specimen face with the y axis aligned vertically along the specimen length. Figure 3 shows a typical Hencky strain distribution for the ϵ_{yy} strain for a single image after necking. The colors designate different contours of strain.

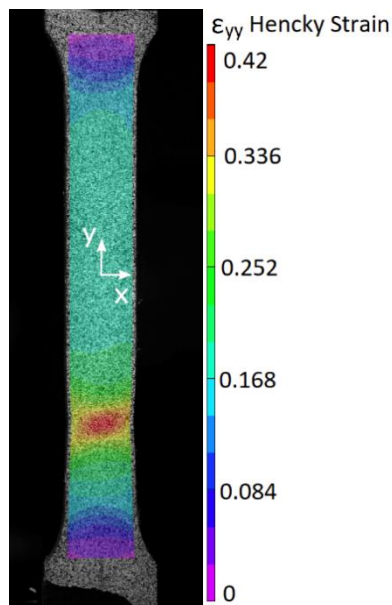


Figure 3: An example of a strain contour plot of a typical test after necking [E191210-ERR-331-1108].

The DIC correlation is run with each image being compared against an original reference image at the start of the test. Near the end of the test in the high strain regions of the specimen, some points will not correlate. When this starts to occur, the correlation mode is manually changed to 'incremental'; each image is compared to the previous image instead of the original reference image. In most tests, about 10 of the final images are run in incremental correlation mode. For each test, the specific image number for the transition to incremental correlation can be found in the summary table file (see Section 4.2). In some cases the start of incremental correlation was not recorded and those are shown as 'not recorded' in the file.

² Certain commercial equipment, instruments, or materials are identified in this report in order to specify the experimental procedure adequately. Such identification is not intended to imply recommendation or endorsement by the National Institute of Standards and Technology, nor is it intended to imply that the materials or equipment identified are necessarily the best available for the purpose.

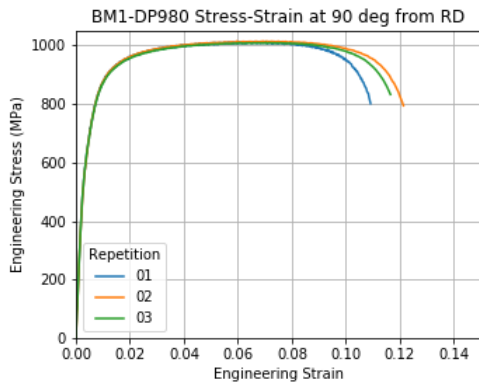
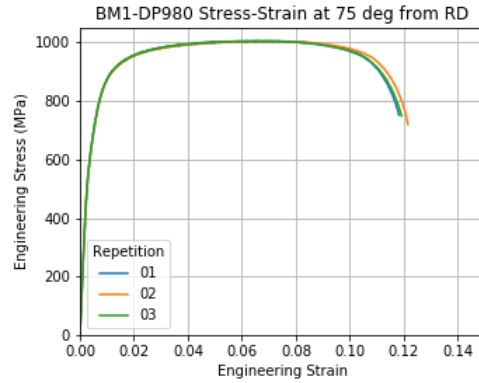
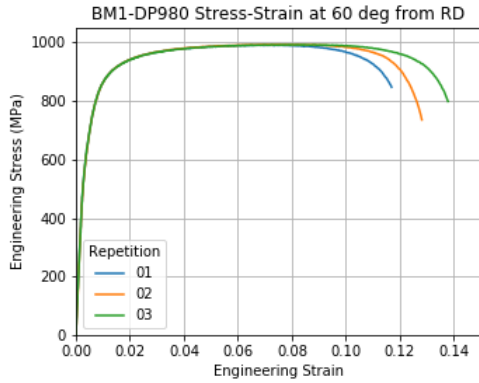
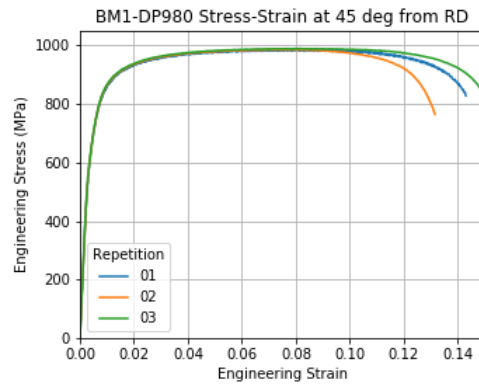
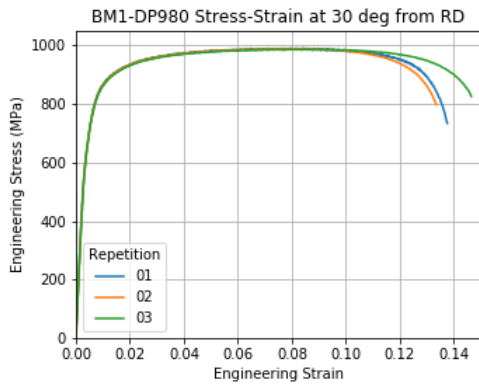
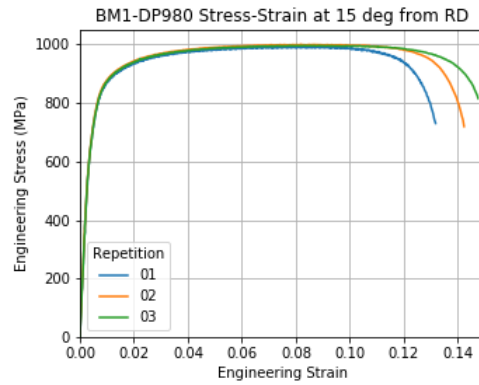
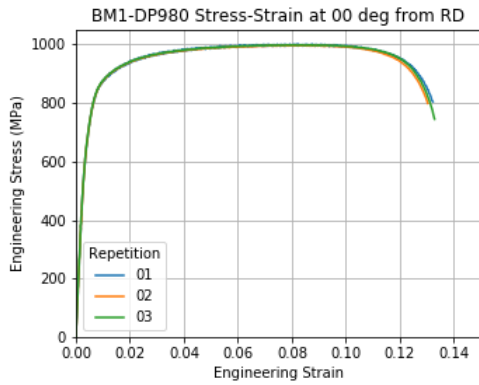
The output of each test is a strain profile of the local centerline Hencky strain at each individual time step. The area of interest (AOI) encompasses the entire reduced parallel section of the test specimen plus a small amount extending past each fillet. In all files, the X direction is horizontal. The Y direction is vertical and is the tensile stretch axis. For each acquired image, the deformed coordinates (X, Y, Z) and Hencky strain points ($\epsilon_{xx}, \epsilon_{yy}, \epsilon_{xy}$) are written to an output file for 201 points spaced 0.25 mm apart along the vertical centerline from an area of interest centered on the reduced parallel length of the specimen (see Section 4.3). They were produced using the Vic-3D “Export metric node data” function.

3. Analysis

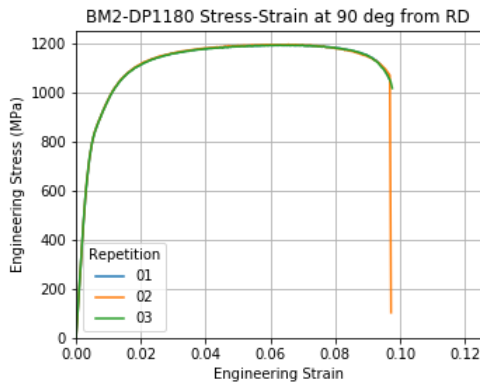
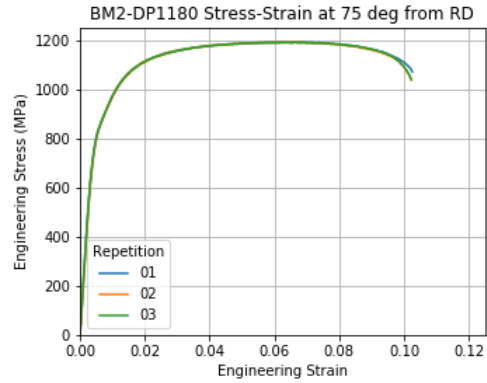
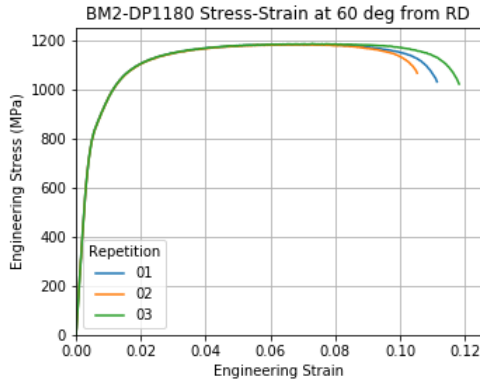
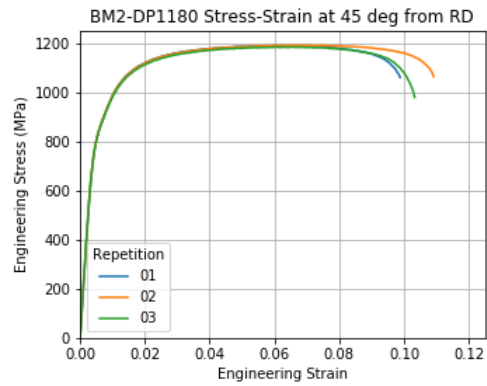
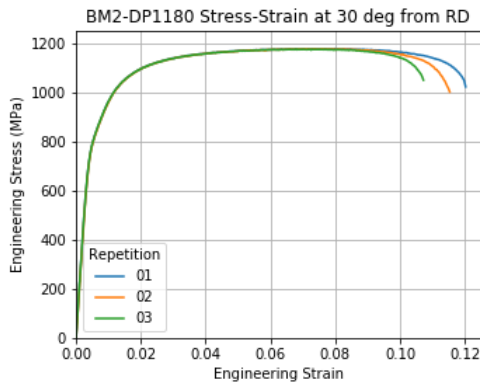
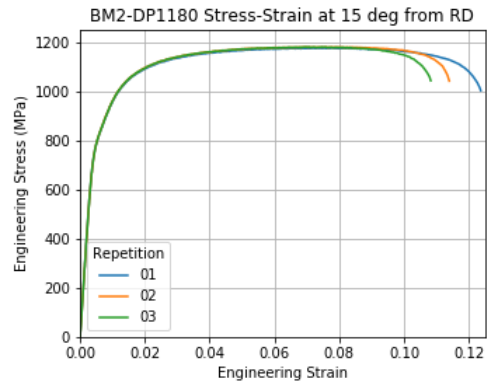
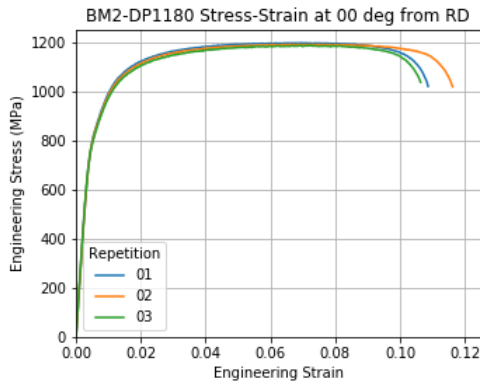
3.1. Engineering stress-strain diagrams

Engineering stress and strain diagrams are provided for reference only. The stress-strain curves shown in this report were created by defining a virtual extensometer with a nominal gauge length, $G = 50$ mm, centered on the reduced parallel length of the specimen. Engineering stress is calculated in the classic method of dividing current force by initial area, based on the average width and thickness measured for each specimen. For each material, the scales of the axes are the same for all seven orientations.

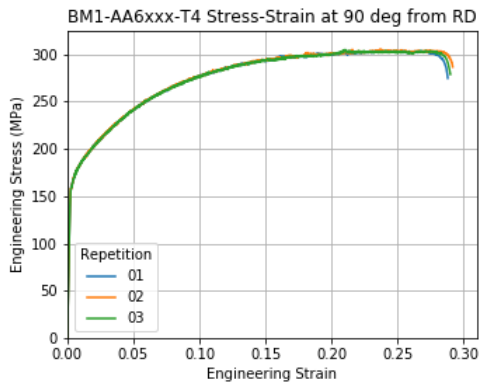
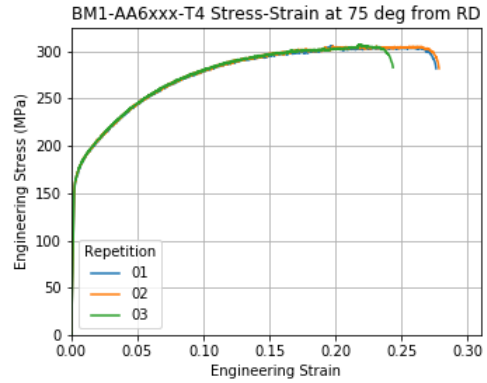
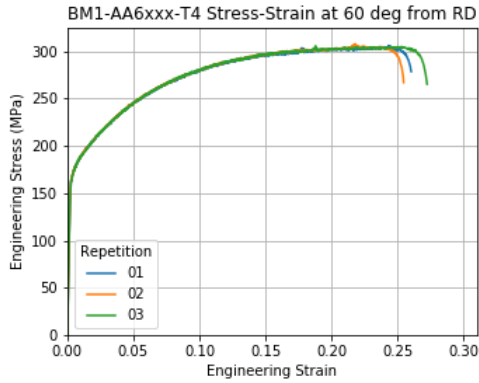
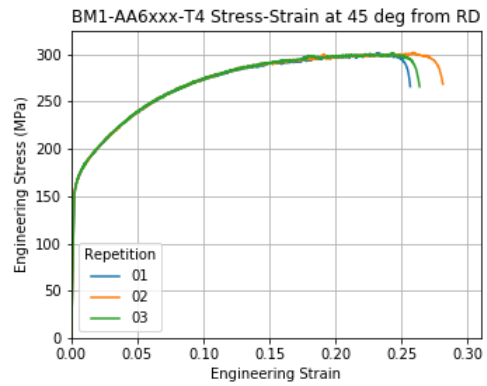
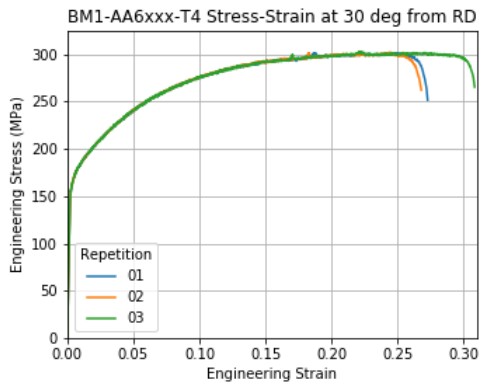
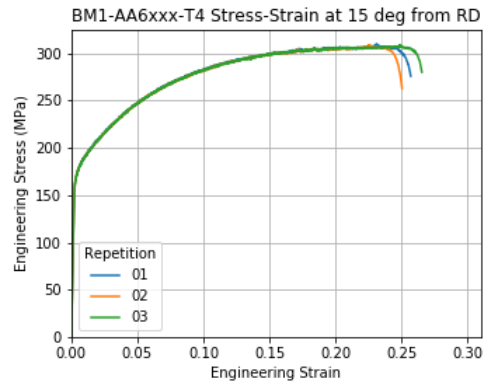
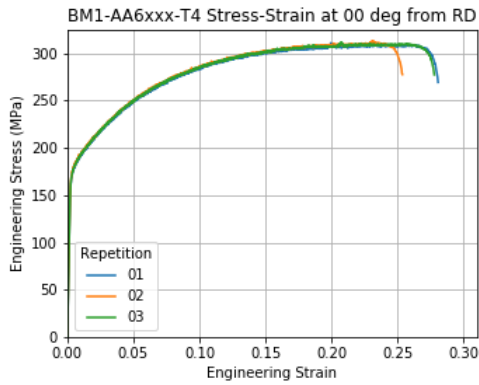
3.1.1. BM1-DP980 engineering stress strain curves



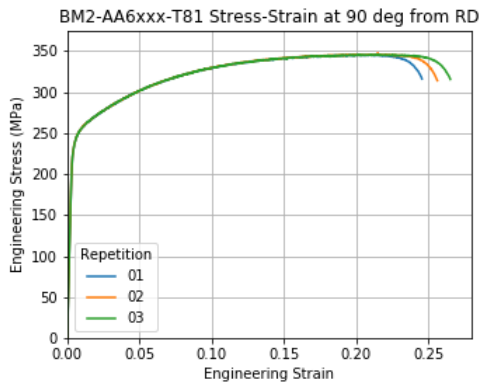
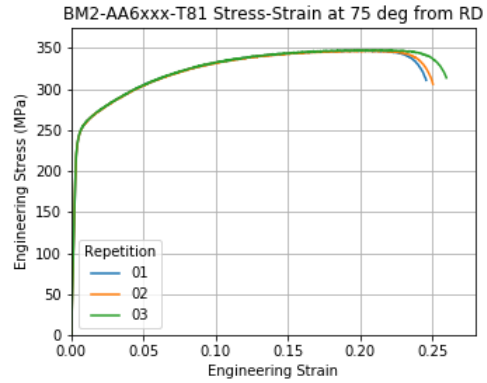
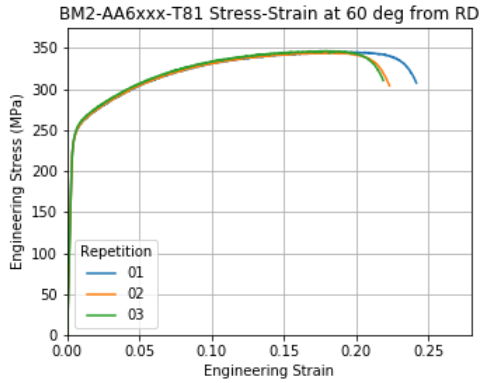
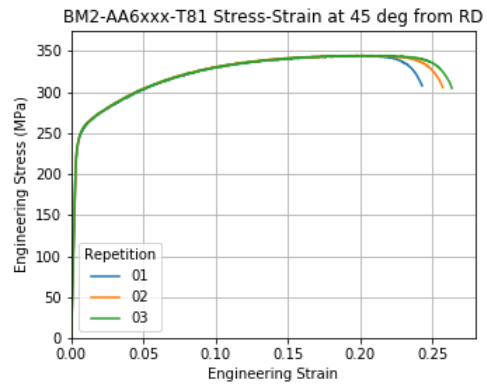
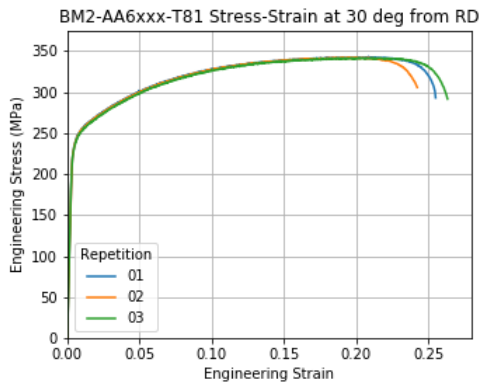
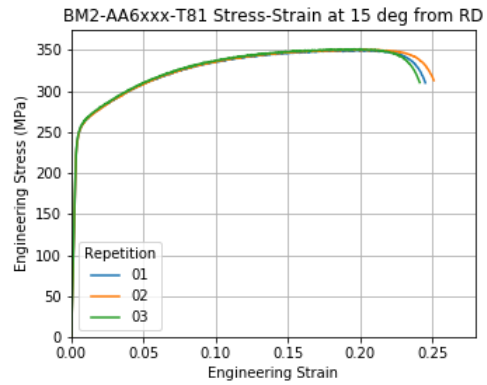
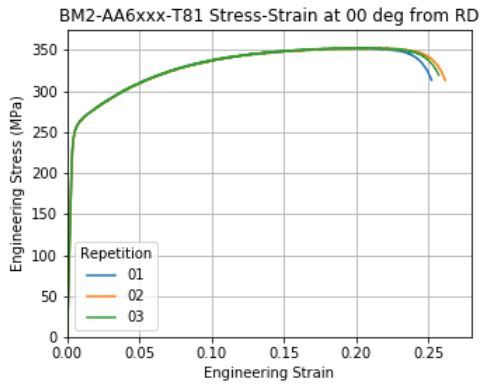
3.1.2. BM2-DP1180 engineering stress strain curves



3.1.3. BM1-6xxx-T4 engineering stress strain curves



3.1.4. BM2-6xxx-T81 engineering stress strain curves



4. Appendixes

4.1. Naming Convention

DIC measured strain profile data are written in a comma-separated value file using a naming convention that captures the deformation mode, orientation, material, and test specimen dimensions as explained in Table 1.

4.2. Format of the uniaxial test summary table file

The uniaxial test summary table file (“Numisheet 2020 Uniaxial Tension Test Summary Table.csv”) contains information about each test including file names, NCAL data base identifier, measured geometry, noise floor, and DIC image numbers of note, see Table 2. Column descriptions for tensile test summary table file (“Numisheet 2020 Uniaxial Tension Test Summary Table.csv”).

4.3. Format of the local-strain files

Strain profiles are included that contain a strain trace running on the centerline of the specimen for each experimental point on the stress-strain curve. Appendix 4.1 describes the naming convention. The strain profile was exported using the Vic-3D function “Export metric node data”. The trace of sextuples (X , Y , Z , ϵ_{xx} , ϵ_{yy} , ϵ_{xy}) was interpolated for $X = 0$ mm (i.e., along the vertical centerline) at 0.25 mm intervals in the range $-25 \text{ mm} \leq Y \leq 25 \text{ mm}$, so the file contains $((50 \text{ mm}/(0.25 \text{ mm/point})) + 1) \times 6 = 1206$ columns of position and strain data. Figure 4 below shows where these interpolated points are located on the specimen. The (X , Y , Z) are deformed coordinates, and the strains (ϵ_{xx} , ϵ_{yy} , ϵ_{xy}) are the Hencky true strains.

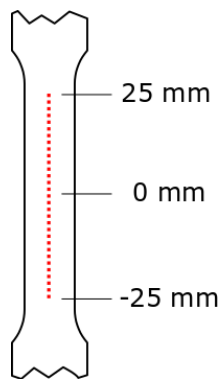


Figure 4. Data point locations on specimen length.

Following those 1206 columns are the analog signal columns; analog signals (e.g., Force) from the test frame are captured during the test, as summarized in Table 3. Engineering stresses can be calculated from the included force, and from the original test specimen dimension encoded in the file name. Engineering strains can be calculated for any arbitrary gauge length from the deformed coordinates. Note that the exported interpolated position and strain data are spaced about 8 times more closely than the size of the virtual strain gauge.

4.4. Stereo-DIC system hardware

The stereo-DIC hardware were configured in three different setups, and the setup used for each test is noted in the summary table file, see Section 4.2. Table 4 summarizes these three setups. A fan was used

after Setup 1 to break up undesirable heat currents that were somewhat noticeable at low strains with Setup 1. Setup 3 added cross-polarization between the light source and cameras to mitigate the specular reflections of the aluminum samples, and cameras were repositioned for a larger field of view to allow for the larger total elongation of the aluminum materials. Setup 3 is shown in Figure 2.

Table 1: Example file naming convention for a strain profile data file (e.g., U00FeDP1180_Numisheet2020R01T1.022W12.66.csv).

Entry	Description
U	Test type: U=uniaxial
00	Angle to the rolling direction in degrees, limited to two digits
Fe	Major alloy component: Fe or Al
DP1180	Alloy type. DP1180, DP980, 6XXX-T81, or 6XXX-T4
_Numisheet2020	Open space for other descriptive information
R01	Repetition number from this test, in this case 01
T1.022	Specimen thickness in mm, in this case 1.022 mm
W12.66	Specimen thickness in mm, in this case 12.66 mm
.csv	File type identifier

Table 2. Column descriptions for tensile test summary table file (“Numisheet 2020 Uniaxial Tension Test Summary Table.csv”).

Column Head	Description
File Name	File Name (see section 4.1)
Material	Material Identifier
Angle from RD (deg)	Specimen orientation in respect the sheet rolling direction
Thickness (mm)	Measured specimen thickness before testing, average of three values along the reduced parallel length.
Width (mm)	Measured specimen width before testing, average of three values along the reduced parallel length.
Repeat Number	Test repeat number for specimen material and orientation.
Aluminum Bake Batch	The BM2-AA6xxx-T81 sheet material was baked prior to specimen fabrication. This value identifies which sheet (bake cycle) the test specimen came from for this material.
DIC Setup Number	Three DIC setups were used during the test campaign (see Section 4.4); this identifies which tests were run with which setup.
Reference Img	DIC reference image number
Test Start Img	DIC image number when test begins (setup images are captured before test starts).
Start Incremental Img	Image number when DIC analysis switches to ‘incremental correlation’
Final Img	Last image number before test specimen failure.
Noise Floor e_{xx} , e_{yy} , e_{xy}	DIC noise floor determined (see Section 4.6).
NCAL Database ID	NCAL Internal database identifier
Test Date	Test Date

Table 3: Format of the last columns describing analog signals of the DIC strain profile data files.

Column Head	Description
Count	Image Count
Time_0	Time from camera 0 in seconds
Time_1	Time from camera 1 in seconds
Dev2/ai0	Unscaled voltage values, ignore
Dev2/ai1	Unscaled voltage values, ignore
Dev2/ai2	Unscaled voltage values, ignore
Dev2/ai3	Unscaled voltage values, ignore
Displacement_(mm)	Actuator displacement in mm
Force_(kN)	Force in kN measured from 100kN load cell
Extensometer	Ignore
unused	Ignore

Table 4: Summary of the stereo-DIC hardware, setup, and analysis used for the uniaxial tension tests.

Hardware and Setup	Setup 1	Setup 2	Setup 3
Cameras	5 MP Point Grey Grasshopper 50S5M-C (2448 pixel x 2048 pixel)		
Lenses	35 mm Schneider Xenoplan		
Standoff	430 mm		480 mm
Lighting	White LED array		Cross-polarized LED array and lens filters
Fan	None	Yes	
Stereo Angle	30 degrees	19 degrees	
Image Scale	26 pixels/mm	27 pixels/mm	24 pixels/mm
Field of View (vertical)	94 mm	91 mm	102 mm
Exposure Time	3.5 ms	3 ms	38 ms
Aperture	f# 6		
Frame rate	(0.5 – 1) Hz		
Camera Interface	Firewire		
DIC Analysis Setting			
Subset	23		21
Step	8		7
Subset shape function	Affine		
Strain Calculation	Hencky		
Strain-filter size	5		
Virtual strain gauge (VSG) size	55 pixels (2.11 mm)	55 pixels (2.04 mm)	49 pixels (2.04 mm)
VSG equation	$(\text{strain-filter size} - 1) * \text{step} + \text{subset}$		

4.5. Virtual strain gauge sensitivity analysis

The analysis parameters used during the processing of the DIC images have a significant effect on both the noise-floor and the maximum measurable strain gradients. Since the longitudinal strain is the primary quantity in the representation of the stress-strain response, this quantity of interest will be the focus of the effects of the DIC analysis parameters. The process of selecting a judicious set of DIC analysis parameters is often referred to as a virtual strain gauge (VSG) study, and is described in A Good Practices Guide for DIC reference [3]. The results of this process will vary with changes in the hardware and setup of the DIC system and/or changes in the DIC pattern used. Although one patterning method was used for all the uniaxial tension tests described here, however three different stereo-DIC setups were used, see Section 4.4. Therefore, three different VSG studies were performed and they are presented here. Three key parameters (subset size S_{ss} , step size S_{st} , and strain-filter size F) are varied during the VSG study. The Good Practices Guide [3] combines these independent length variables into a single value parameter (VSG), the VSG size which is defined as,

$$S_{VSG} = S_{ss} + (F - 1) S_{st}$$

and is used to estimate the length over which the strain is calculated. Smaller VSG lengths typically results in larger strain noise but better-resolved strain gradients, while larger VSG lengths typically results in smaller strain noise but more smoothed strain gradients. Figure 5 provides a visual comparison between the strain noise for large and small VSG lengths on the same image. An informed balance between the two desirable but competing outcomes (low strain noise versus better-resolved strain gradients) is the goal of the VSG study.

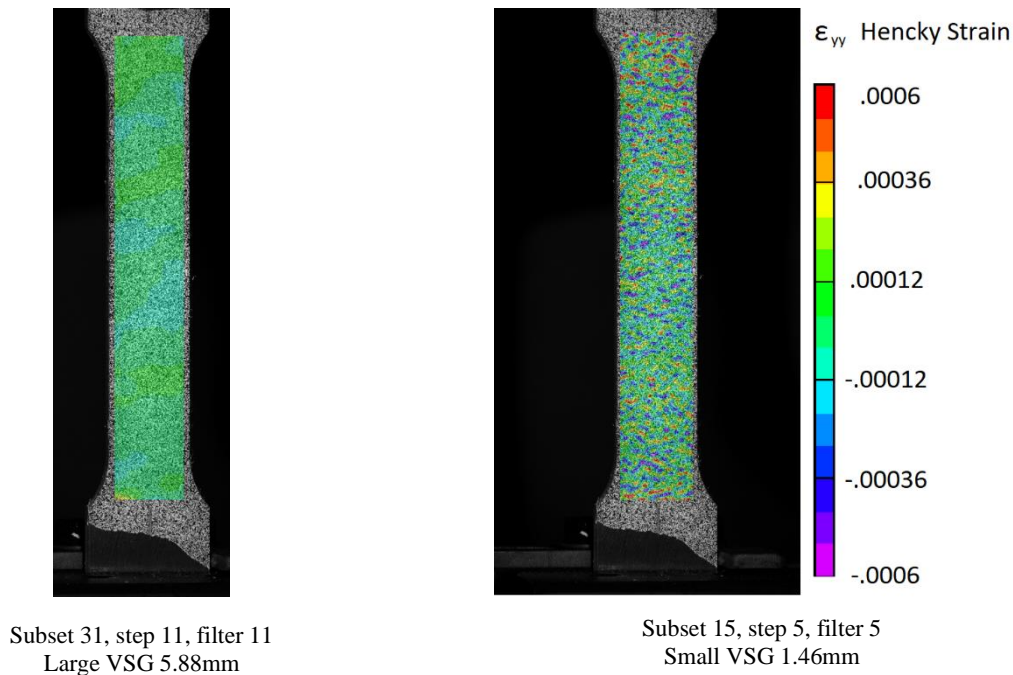


Figure 5: ϵ_{yy} true strain noise difference visualization between large and small VSG sizes [E191210-ERR-311].

For each stereo-DIC setup (Table 4), one representative test was selected to perform a detailed VSG study for that setup. In each VSG study, one image from the pre-load phase and one image from just before failure was selected. These images were analyzed using a variety of subset, step, and filter size combinations, resulting in VSG lengths between 30 pixels and 325 pixels.

The spatial strain noise was assessed using all correlated data points from a pre-load image, where strain is known to be zero. Although the mean strain value in each case was not zero, the standard deviation of the strain was significantly larger than the mean. Therefore, the VSG study assessed the strain noise based on just the standard deviation of the strain. Figure 6(a), Figure 7(a), and Figure 8(a) plot one standard deviation of the strain for each VSG size that are the result for various combinations of subset size, step size, and filter size. In each case, the smaller the VSG size the larger the standard deviation of strain. VSG size was calculated in pixel, and then converted to mm based on the image scale (Table 4).

For each test, the near failure image is presumed to have the highest strain gradient as the strain is localizing prior to failure, and this image is used to assess the spatial smoothing. Figure 6(b), Figure 7(b), and Figure 8(b) show the local strain behavior along the reduced parallel length for three representative VSG sizes. These profiles are color coded to the three matching points in the other parts of each figure. The peak strain value in each profile was assessed at the same location (*Y* position) along the length of the profile for all the VSG sizes analyzed and is plotted versus the VSG size in part (c) of each figure. In each case, the larger the VSG size the more the peak strain is smoothed.

The tradeoff between the local strain noise and smoothing of the peak strain value for all the VSG sizes considered in each study is summarized in part (d) of Figure 6, Figure 7, and Figure 8. The green, red and blue data points and the associated strain profiles represent three potential outcomes of the VSG study. The green data point and profile demonstrate a VSG selection that will result in smaller local strain noise but more smoothing of the higher strain gradients. This could be desirable if only the low strain behavior is of interest and noise had to be minimized. The blue data point and profile demonstrate a VSG selection that will result in minimal reduction of the peak strain near failure, but at the cost of a larger strain noise. This could be desirable if the strain near failure is the critical measurement. The red data point and profile was selected based on the desire to capture as high a strain as possible while keeping the local noise between 125 $\mu\text{m}/\text{mm}$ and 150 $\mu\text{m}/\text{mm}$, and it demonstrates a balance between capturing much of the high strain behavior while restricting the local strain noise. The parameters associated with the red data points were selected as the optimum for each setup and are summarized in Table 3.

4.5.1. DIC Setup 1

The experiment [E191022-ERR-103] is used for the VSG study for DIC Setup 1 [L200324-ERR-001]. The preload image 10 and near failure image 600 are used for the strain noise and peak strain smoothing assessments, respectively. The results are presented in Figure 6. The parameters selected based on this VSG study coincide with the red data points and curve shown in the figure. Based on the VSG results strains near 0.395 mm/mm measured with Setup 1 should be considered a lower bound of the actual strain values.

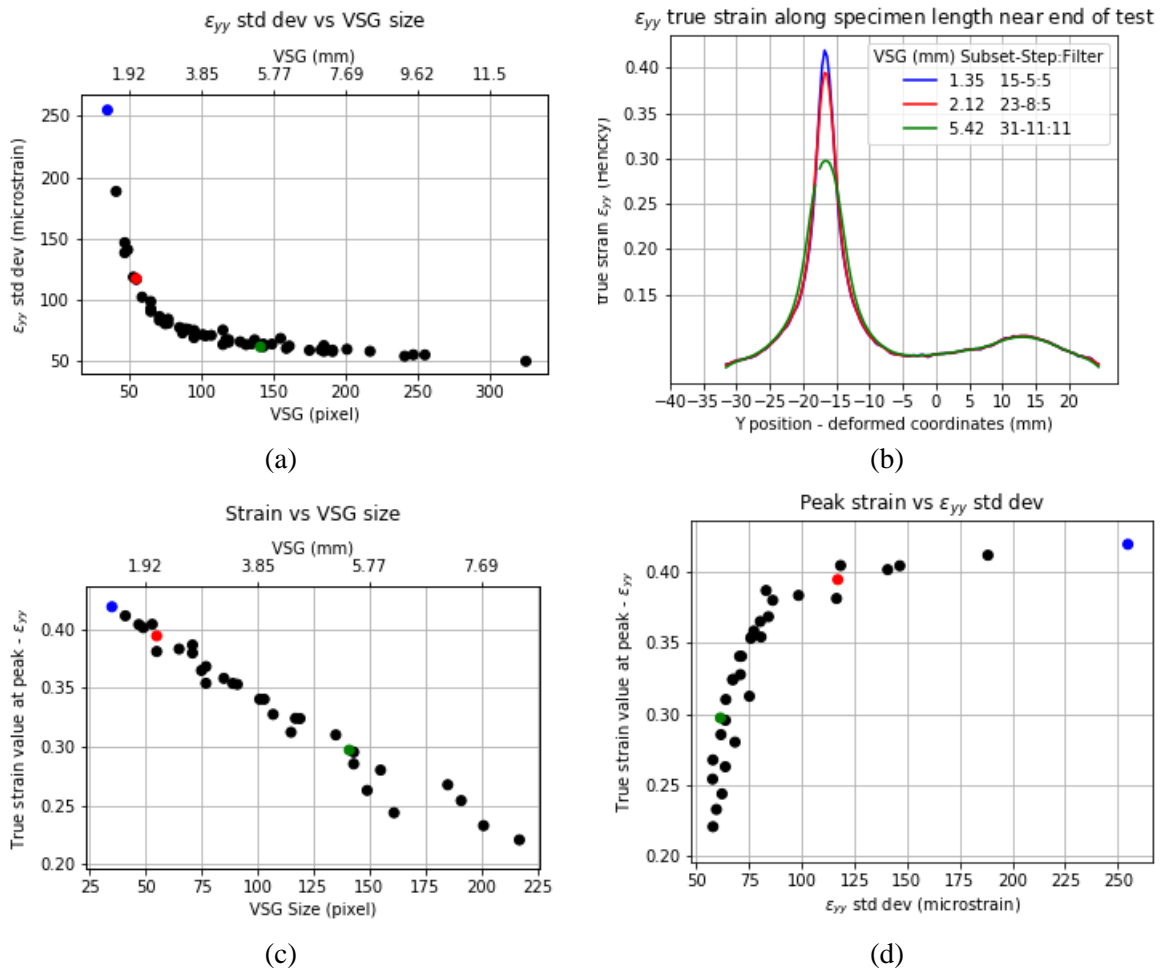


Figure 6: Virtual strain gauge study results for DIC Setup 1. (a) spatial noise versus VSG length, (b) strain profiles for three selected VSG lengths (the profiles are color coded to the three matching VSG lengths in the other parts of the figure), (c) peak profile strain versus VSG length, (d) peak profile ϵ_{yy} versus spatial noise.

4.5.2. DIC Setup 2

The experiment [E191119-ERR-003] is used for the VSG study for DIC Setup 2 [L200324-ERR-001]. The preload image 21 and near failure image 528 are used for the strain noise and peak strain smoothing assessments, respectively. The results are presented in Figure 7. The parameters selected based on this VSG study coincide with the red data points and curve shown in the figure. Based on the VSG results strains near 0.255 mm/mm measured with Setup 2 should be considered a lower bound of the actual strain values.

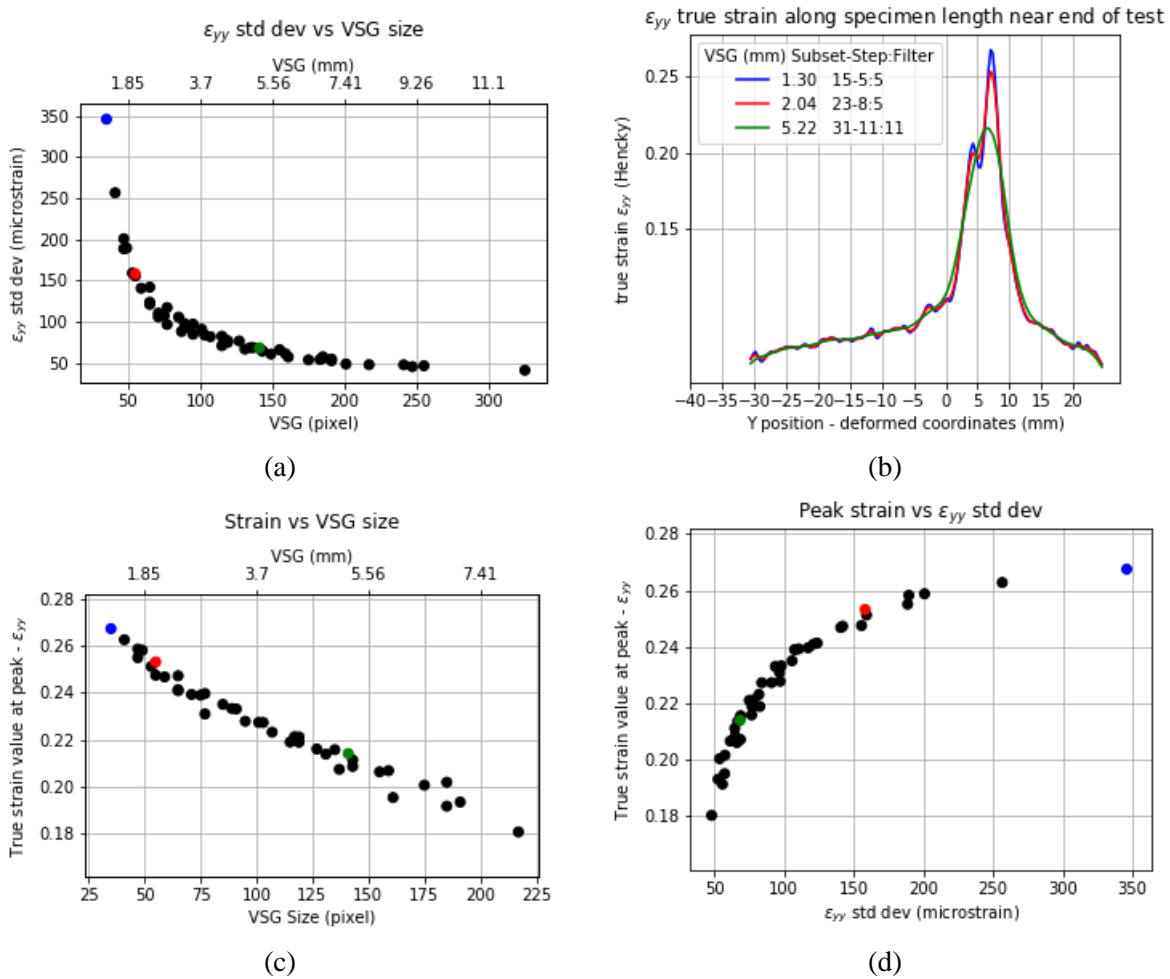


Figure 7: Virtual strain gauge study results for DIC Setup 2. (a) spatial noise versus VSG length, (b) strain profiles for three VSG selected lengths (the profiles are color coded to the three matching VSG lengths in the other parts of the figure), (c) peak profile strain versus VSG length, (d) peak profile strain versus spatial noise.

4.5.3. DIC Setup 3

The experiment [E191210-ERR-311] is used for the VSG study for DIC Setup 3 [L200324-ERR-001]. The preload image 12 and near failure image 1108 are used for the strain noise and peak strain smoothing assessments, respectively. The results are presented in Figure 8. The parameters selected based on this VSG study coincide with the red data points and curve shown in the figure. Based on the VSG results strains near 0.415 mm/mm measured with Setup 3 should be considered a lower bound of the actual strain values.

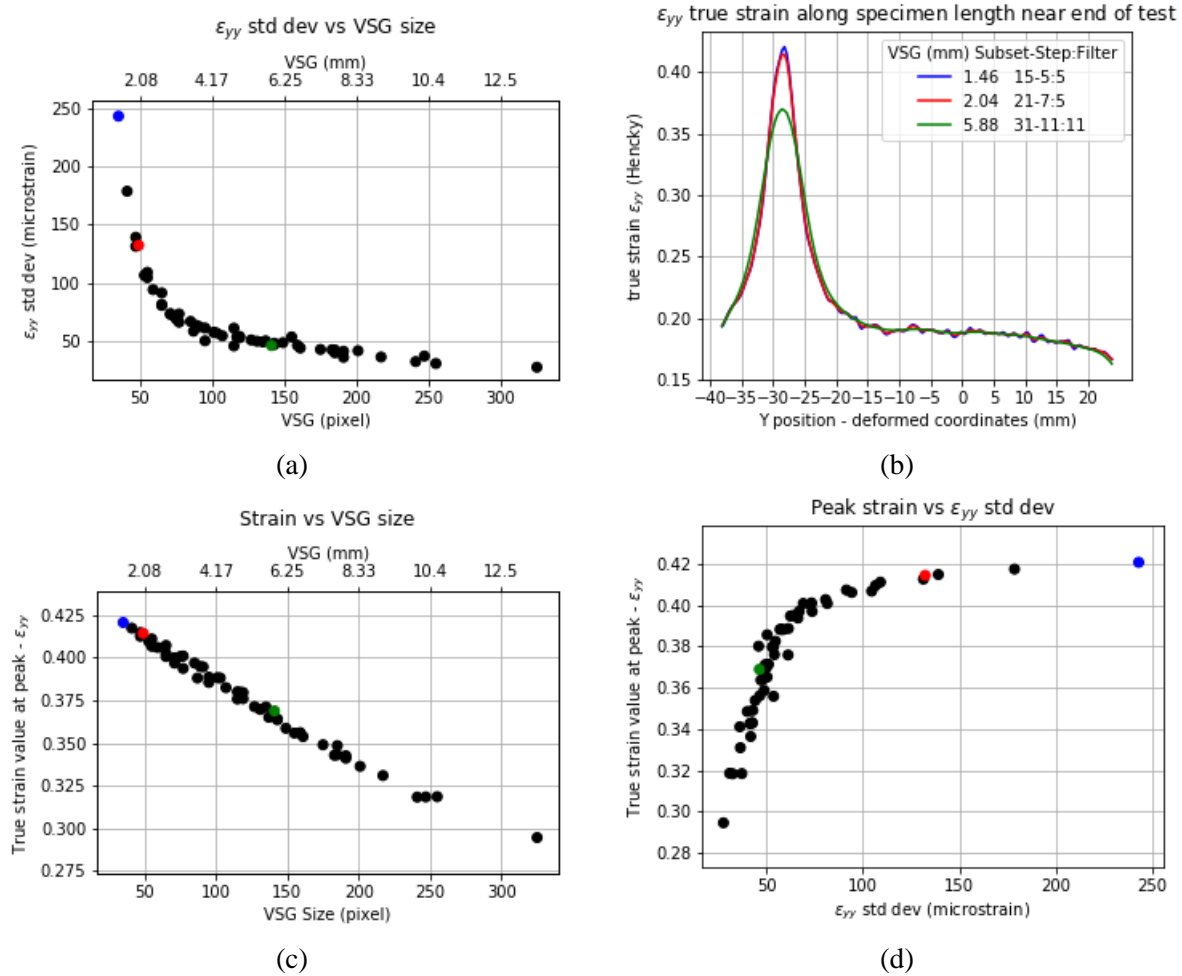


Figure 8: Virtual strain gauge study results for DIC Setup 3. (a) spatial noise versus VSG length, (b) strain profiles for three VSG selected lengths (the profiles are color coded to the three matching VSG lengths in the other parts of the figure), (c) peak profile strain versus VSG length, (d) peak profile strain versus spatial noise.

4.6. Noise-floor analysis

At the start of each test, but before any actuator motion, the data acquisition system captured several static images. Five of these static images were used to estimate the noise-floor for each test. The results are presented in the uniaxial test summary table file (see Section 4.2). The noise-floor value was used as a simple quality metric to determine if there was any outlier behavior in the DIC system, calibration, or patterning. The reported true strain noise-floor values, n_ϵ , are calculated using the mean and standard deviation (std) of each of the images as

$$n_\epsilon = |\text{mean}(\epsilon)| + \text{std}(\epsilon)$$

for each component of strain. The value reported for each test is the worst value of the five images for that test. In each test, the majority of the noise floor comes from the spatial variation in strain expressed in the standard deviation, rather than from the change in the mean value.

4.7. NCAL information

This report and data are archived as NCAL collate ID L200326-ERR-001.

5. References

- [1] ASTM International. Standard practice for verification of testing frame and specimen alignment under tensile and compressive axial force application. Standard E1012-14e1, ASTM International, W. Conshohocken, Pa, 2012. doi:10.1520/E1012-14E01.
- [2] ASTM International. E8/E8M-16a Standard Test Methods for Tension Testing of Metallic Materials. West Conshohocken, PA, 2016. doi:10.1520/E0008_E0008M-16A.
- [3] E. M. C. Jones and M. A. Iadicola, editors. *A Good Practice Guide for Digital Image Correlation*. International Digital Image Correlation Society, 2018. doi:10.32720/idics/gpg.edl.